Aug 24th, 12:00 AM - Aug 25th, 12:00 AM

Behaviour of LiteSteel Beams Subject to Combined Shear and Bending Actions

P. Keerthan

D. Hughes

M. Mahendran

Twenty-First International Specialty Conference on Cold-Formed Steel Structures
St. Louis, Missouri, USA, October 24 & 25, 2012

Behaviour of LiteSteel Beams Subject to Combined Shear and Bending Actions

P. Keerthan[1], D. Hughes[2] and M. Mahendran[3]

Abstract

This paper presents the details of a numerical study of a cold-formed steel beam known as LiteSteel Beam (LSB) subject to combined shear and bending actions. The LSB sections are produced by a patented manufacturing process involving simultaneous cold-forming and electric resistance welding. They have a unique shape of a channel beam with two rectangular hollow flanges. To date, however, no investigation has been conducted into the strength of LSB sections under combined shear and bending actions. Hence a numerical study was undertaken to investigate the behaviour and strength of LSBs subject to combined shear and bending actions. In this research, finite element models of LSBs were developed to simulate the combined shear and bending behaviour and strength of LSBs. They were then validated by comparing their results with test results and used in a parametric study. Both experimental and finite element analysis results showed that the current design equations are not suitable for combined shear and bending capacities of LSBs. Hence improved design equations are proposed for the capacities of LSBs subject to combined shear and bending actions.

Keywords: *LiteSteel beams, Combined shear and bending actions, Finite element analyses, Experiments, Cold-formed steel structures, Slender web, Hollow flanges.*

1. Introduction

The use of cold-formed steel members in low rise building construction has increased significantly in recent times. There are many significant benefits associated with the use of lightweight cold-formed steel sections in buildings.

[1] Post-doctoral Research Associate, [2]Research Student and [3]Professor, Science and Engineering Faculty, QUT, Australia.

LiteSteel beam (LSB) is a hollow flange channel section marketed primarily for use as a flexural member in residential and commercial/industrial applications (Figure 1) (OATM, 2008). It is manufactured from a single strip of high strength steel through the use of a combined cold-forming and dual electric resistance welding process. The effective distribution of steel in LSBs with two rectangular hollow flanges results in a lightweight section with good moment capacity.

Figure 1: LiteSteel Beam (OATM, 2008)

Many studies have been conducted into the structural behaviour and design of the LSB. However, no investigation has been conducted into the strength of LSB sections under combined shear and bending actions. Combined shear and bending is especially prevalent at the supports of continuous span and cantilever beams, where the interaction of high shear force and bending moment can reduce the capacity of a section to well below that for the same section subject only to pure shear or moment. The behaviour of steel beams in combined shear and bending has been investigated by many researchers, including LaBoube and Yu (1978), Bleich (1952), Evans (1983), and Shahabian and Roberts (2008), with provisions for the design of members subject to such loading included in both AS/NZS 4600 (SA, 2005) and AS 4100 (SA, 1998). Currently the design of LSBs is governed by the cold-formed steel structures code, AS/NZS 4600.

AS/NZS 4600 (SA, 2005) recommends a circular interaction equation for the design of flexural members subject to combined shear and bending actions. LaBoube and Yu (1978) performed an experimental investigation of the combined shear and bending behaviour of cold-formed channel sections without transverse stiffeners, and identified that a circular relationship for shear and bending interaction is quite conservative. The circular equation was originally derived for individual disjointed plates in combined bending and shear, and is not accurate when applied to webs restrained by flanges. This is likely to be especially true for the LSB given the significant rigidity of its flanges.

Most studies concerned with combined shear and bending have focused on hot-rolled plate girders or cold-formed members with open flanges rather than hollow flanges. Keerthan and Mahendran (2011) have shown that the flanges of the LSB provide nearly fixed restraint to the web, which has a significant effect on its shear buckling coefficient and post-buckling strength. AS/NZS 4600, however, currently considers only simply supported conditions at the edges of the web panel, and ignores the available post-buckling capacity in shear. An investigation of LSBs subject to combined shear and bending actions was therefore undertaken using numerical studies to develop improved design rules. This paper presents the details of the numerical studies into the structural behaviour and design of LSBs subject to combined shear and bending actions.

2. Finite Element Modelling

2.1. Model Details

This section describes the finite element model used to evaluate the strengths and behaviour of LSB sections subject to combined shear and bending actions. A finite element program, ABAQUS Version 6.7 (HKS, 2007), which has the capability of undertaking geometric and material non-linear analyses of three dimensional structures, was used. Finite element models were first developed to simulate the behaviour of 18 simply supported back to back LSBs tested under a three-point loading arrangement shown in Figure 2. Appropriate parameters were chosen in these models for the geometry, mechanical properties, loading and support conditions, initial geometric imperfections, and residual stresses.

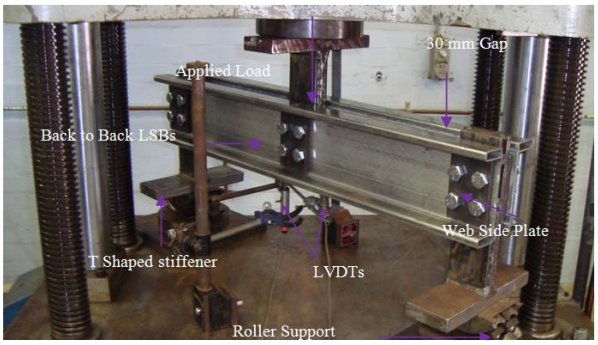

Figure 2: Experimental Set-up

Shear tests gave very similar results when back to back LSBs or single LSBs with a shear centre loading were used. Hence in this study, finite element models of single LSBs with shear centre loading and simply supported boundary

conditions were used to simulate the combined shear and bending tests of back to back LSBs. The cross-section geometry of the finite element model was based on the measured dimensions and yield stresses of tested LSBs. Table 1 gives the measured dimensions and yield stresses of the test specimens. In this table t_w and d_1 are the base metal thickness and the clear web height, and f_{yo}, f_{yi} and f_{yw} are the yield stresses of outside flange, inside flange and web, respectively.

Table 1: Details of LSB Test Specimens

No.	LSB Section	Aspect Ratio	d_1 (mm)	Yield stress (MPa)			Thickness (mm)			Flange width (mm)	Flange depth (mm)
				f_{yo}	f_{yi}	f_{yw}	Outside Flange	Inside Flange	Web t_w		
1	150x45x1.6	2.0	121.3	558	488	454	1.77	1.66	1.60	45.4	14.8
2	150x45x1.6	2.5	120.0	558	488	454	1.76	1.66	1.58	45.6	14.7
3	150x45x1.6	3.0	120.1	558	488	454	1.78	1.65	1.58	45.4	14.8
4	150x45x1.6	3.5	120.0	558	488	454	1.77	1.66	1.58	45.5	14.9
5	150x45x1.6	3.9	120.0	558	488	454	1.77	1.67	1.58	45.4	14.8
6	150x45x2.0	2.0	121.2	538	492	423	2.25	2.08	1.99	45.5	14.8
7	150x45x2.0	2.5	120.0	538	492	423	2.25	2.09	1.97	45.6	14.9
8	150x45x2.0	3.0	120.0	538	492	423	2.24	2.08	1.98	45.5	14.8
9	150x45x2.0	3.5	120.9	538	492	423	2.26	2.07	1.97	45.4	14.7
10	150x45x2.0	3.9	120.0	538	492	423	2.25	2.08	1.97	45.5	14.8
11	200x45x1.6	2.0	170.0	537	491	452	1.66	1.61	1.58	45.6	15.3
12	200x45x1.6	2.5	169.6	537	491	452	1.66	1.60	1.58	45.4	15.0
13	200x45x1.6	3.0	170.7	537	491	452	1.68	1.61	1.58	45.5	15.1
14	200x45x1.6	4.0	170.8	537	491	452	1.67	1.60	1.59	45.4	14.9
15	200x60x2.0	2.0	161.5	521	471	440	2.12	2.02	1.96	59.9	20.4
16	200x60x2.0	3.5	160.0	521	471	440	2.10	2.01	1.97	59.9	20.5
17	250x60x2.0	2.0	212.2	523	473	452	2.19	2.04	1.97	60.2	20.7
18	250x60x2.0	3.0	211.8	523	473	452	2.20	2.03	1.99	60.1	20.7

Note: Aspect Ratio = Shear span/ Clear height of web

Finite element models were developed using centreline dimensions and ignoring corner radii. Since the effect of including the rounded corners in LSBs on the shear buckling behaviour and capacity was found to be negligible (Keerthan and Mahendran, 2010), right angle corners were used in the finite element models used in this study. Shell elements were used to simulate the behaviour of LSB sections. The element defined as S4R5 in ABAQUS was selected for all finite element models. The S4R5 element is a thin, shear flexible, isoparametric

quadrilateral shell with four nodes and five degrees of freedom per node, and utilises reduced integration and bilinear interpolation schemes. R3D4 rigid body elements were used to simulate the restraints and loading in the finite element models of LSB. The R3D4 element is a rigid quadrilateral with four nodes and three translational degrees of freedom per node. Convergence studies showed that an element size of 5 mm x 10 mm provided an accurate representation. All the models were therefore constructed with a 5 mm x 10 mm mesh. The geometry and finite element mesh of a typical LSB is shown in Figure 3.

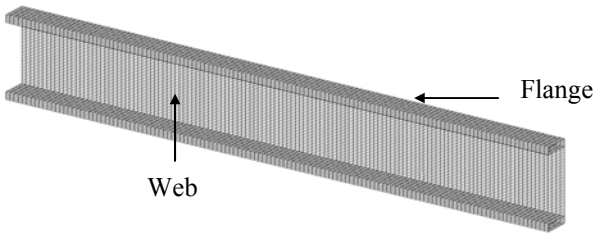

Figure 3: Geometry and Finite Element Mesh of a Typical LSB

2.2. Material Model and Properties

The ABAQUS classical metal plasticity model was used for all the analyses. This model implements the von Mises yield surface to define isotropic yielding, associated plastic flow theory, and either perfect plasticity or isotropic hardening behaviour. A perfect plasticity model was adopted for all the finite element models. The yield stresses obtained from tensile coupon tests were used in the finite element analyses. The elastic modulus and Poisson's ratio were taken as 200,000 MPa and 0.3, respectively. Nominal web and flange yield strengths of 380 and 450 MPa were adopted in the parametric study.

2.3. Loads and Boundary Conditions

Simply supported boundary conditions were implemented in the finite element models of LSBs. In order to provide simply supported conditions for the web panel, the following boundary conditions were used.

Left and right supports: $u_x = 0$ $u_y = 1$ $u_z = 1$ $\theta_x = 1$ $\theta_y = 0$ $\theta_z = 0$
Mid-span loading point: $u_x = 1$ $u_y = 0$ $u_z = 1$ $\theta_x = 1$ $\theta_y = 0$ $\theta_z = 0$

In the above, u_x, u_y and u_z are translations and θ_x, θ_y and θ_z are rotations in the x, y and z directions, respectively, 0 denotes free and 1 denotes restrained. The vertical translation was not restrained at the loading point. Figure 4 shows the

applied loads and boundary conditions of the model. Single point constraints and concentrated nodal forces were used in the finite element models to simulate the experimental boundary conditions. In order to prevent twisting, the applied point load and simply supported boundary conditions were applied at the shear centre using rigid body reference node. Shear test specimens included a 75 mm wide plate at each support to prevent lateral movement and twisting of the cross-section. These stiffening plates were modelled as rigid bodies using R3D4 elements. In ABAQUS (HKS, 2007) a rigid body is a collection of nodes and elements whose motion is governed by the motion of a single node, known as the rigid body reference node. The motion of the rigid body can be prescribed by applying boundary conditions at the rigid body reference node. Hence simply supported boundary conditions were applied to the node at the shear centre in order to provide an ideal pinned support.

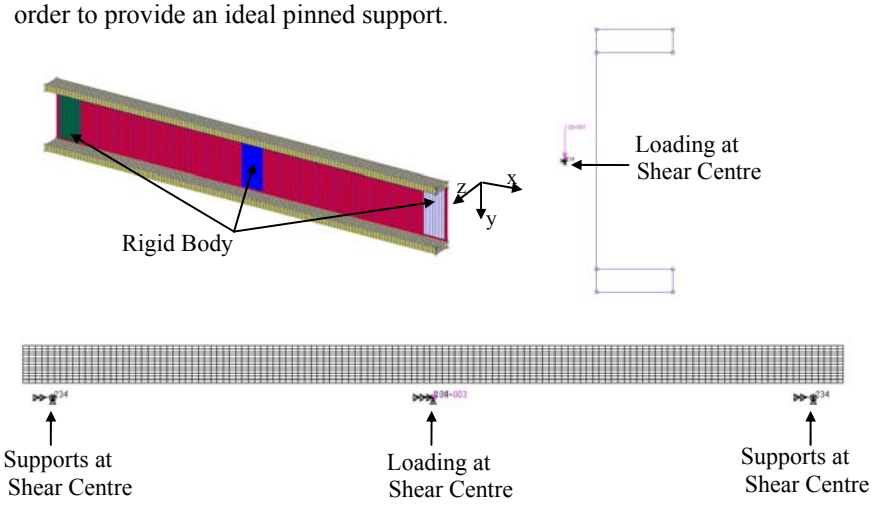

Figure 4: Application of Loads and Boundary Conditions to LSBs

2.4. Modelling of Imperfections

Local plate imperfections were included in all their finite element models using an eigenvector field approach. The magnitude of local imperfections was taken as $d_1/150$ for all the sections. The critical imperfection shape was introduced using the *IMPERFECTION option in ABAQUS. The residual stresses in the new LSB sections produced using the dual electric resistance welding and cold-forming processes have unique characteristics. Details of an idealized residual stress model developed for computer analyses are presented in Seo et al. (2008). To account for the effects of residual stresses, the idealised residual stress distributions shown in Figure 5 were modelled using the *INITIAL

CONDITIONS option in ABAQUS, with TYPE = STRESS, USER. The user defined initial stresses were generated using the SIGINI Fortran user subroutine.

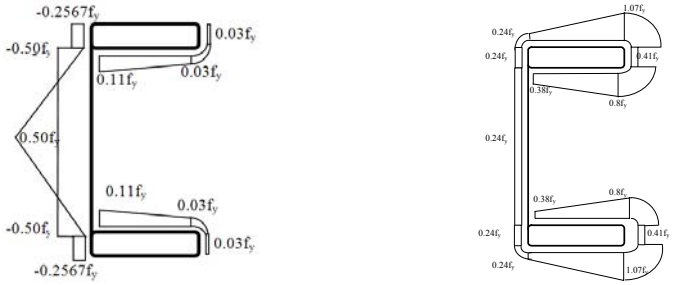

(a) Membrane (b) Flexural

Figure 5: Residual Stress Distributions in 150x45x1.6 LSB (Seo et al., 2008)

2.5. Analysis Methods

The two methods of analysis employed for all FEA investigations were bifurcation buckling and non-linear static analysis. Bifurcation buckling analyses were used to obtain the eigenvectors for the inclusion of geometric imperfections. Non-linear static analyses, including the effects of large deformation and material yielding, were employed to investigate the combined shear and bending behaviour of LSB sections up to failure. The Riks method was included for the non-linear analyses in ABAQUS.

3. Comparison of Finite Element Analysis and Experimental Results

It is necessary to validate the developed finite element models for non-linear analyses of LSBs subjected to combined shear and bending actions. Eighteen models were developed using the material and geometric properties from experiments. In this section, finite element analysis (FEA) results were compared with those from experiments. Table 2 presents a summary of the FEA results of applied mid-span load at failure and a comparison of these results with the corresponding experimental results. The mean and COV of the ratio of test to FEA applied loads are 1.00 and 0.042. This indicates that the finite element model developed in this study is able to predict the ultimate capacity of LSBs subject to combined shear and bending actions with very good accuracy. The failure mechanisms of each of the 18 finite element models also agreed well with those from the experimental study. Figures 6 and 7 show the failure modes of 250x60x2.0 LSB (Aspect Ratio = 2) and 200x45x1.6 LSB (Aspect Ratio = 3). The load-deflection plots from FEA were also compared against those from the

corresponding experimental tests in Figures 8 (a) and 8 (b) for a 250x60x2.0 LSB with aspect ratios of 2.0 and 3.0, respectively.

Table 2: Comparison of FEA and Experimental Results

Test No.	LSB Section	Aspect Ratio (a/d_1)	Applied Load (kN)		Exp/FEA
			Exp.	FEA	
1	150x45x1.6	2.0	178.60	178.80	1.00
2	150x45x1.6	2.5	163.52	170.12	0.96
3	150x45x1.6	3.0	151.60	154.20	0.98
4	150x45x1.6	3.5	133.52	140.40	0.95
5	150x45x1.6	3.9	124.40	125.60	0.99
6	150x45x2.0	2.0	233.92	238.00	0.98
7	150x45x2.0	2.5	207.92	210.00	0.99
8	150x45x2.0	3.0	196.40	195.80	1.00
9	150x45x2.0	3.5	175.20	174.60	1.00
10	150x45x2.0	3.9	157.52	156.00	1.01
11	200x45x1.6	2.0	185.88	178.20	1.04
12	200x45x1.6	2.5	170.24	169.60	1.00
13	200x45x1.6	3.0	155.00	138.40	1.12
14	200x45x1.6	4.0	129.60	124.60	1.04
15	200x60x2.0	2.0	267.08	288.00	0.93
16	200x60x2.0	3.5	208.84	218.00	0.96
17	250x60x2.0	2.0	277.28	288.00	0.96
18	250x60x2.0	3.0	230.36	230.00	1.00

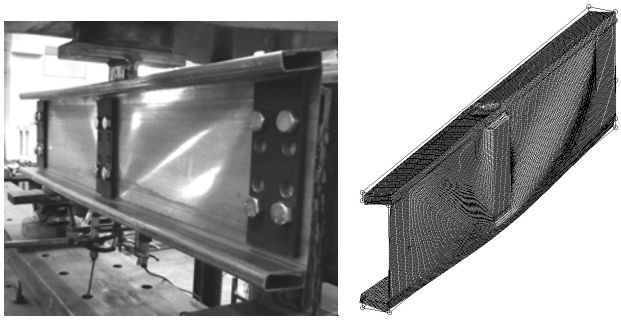

(a)Test (b) FEA)

Figure 6: Failure Mode of 250×60×2.0 LSB (Aspect Ratio = 2.0)

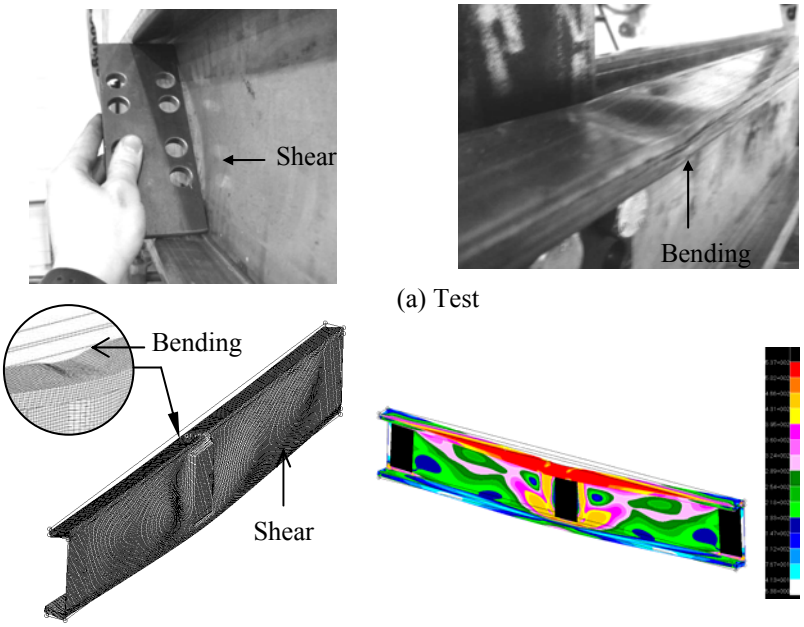

(a) Test

(b) FEA (Deformation) (c) FEA (Stress)

Figure 7: Failure Mode of 200×45×1.6 LSB (Aspect Ratio = 3.0)

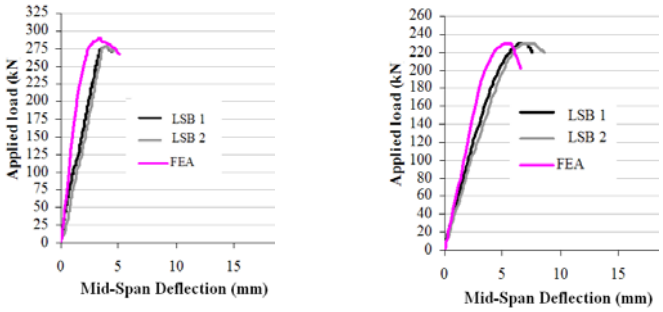

(a) Aspect Ratio =2.0 (b) Aspect Ratio =3.0

Figure 8: Plot of Applied Mid-span Load versus Vertical Deflection (250x60x2.0 LSB)

The FEA load-deflection behaviour agreed reasonably well with test behaviour. These figures demonstrate a good agreement between the results from FEA and experiments and confirm the adequacy of the developed finite element model in predicting the ultimate load, deflections and failure modes of LSBs subjected to combined shear and bending action. Models with aspect ratios of 2.0 displayed primary shear failure modes involving the formation of significant yield zones in the web and only minor flange buckling. Such behaviour is consistent with that observed in tests, particularly as it confirms the development of a post-buckling shear mechanism as observed in the experimental study. Models with aspect ratios of 3.0 showed noticeable flange buckling and yielding.

4. Parametric Study

A detailed parametric study was undertaken based on the validated finite element model to develop suitable design equations for LSBs subjected to combined shear and bending actions. Sixty models were analysed using nominal section dimensions and material properties and aspect ratios of 2.0, 2.5, 3.0, 3.5 and 4.0. Table 3 presents the shear and bending capacity results for LSBs with an aspect ratio of 2.5.

Table 3: Parametric Study Results (Aspect Ratio = 2.5)

LiteSteel Beam Section	a/d_1	Shear Force V (kN)	Bending Moment M(kNm)	Shear Capacity V_u (kN)	Section Moment Capacity M_u (kNm)	V/V_u	M/M_u
300×75×3.0 LSB	2.5	124.5	77.8	150.19	81.9	0.829	0.950
300×75×2.5 LSB	2.5	98.5	61.6	110.24	67.1	0.894	0.917
250×75×3.0 LSB	2.5	117.5	58.8	136.80	65.5	0.859	0.897
250×75×2.5 LSB	2.5	96.5	48.3	103.11	54.0	0.936	0.894
200×60×2.5 LSB	2.5	79.0	31.6	91.20	35.1	0.866	0.900
200×60×2.0 LSB	2.5	61.0	24.4	65.99	27.7	0.924	0.881
200×45×1.6 LSB	2.5	38.6	16.4	45.79	17.5	0.843	0.936
150×45×2.0 LSB	2.5	47.5	14.2	54.72	15.8	0.868	0.901
150×45×1.6 LSB	2.5	36.9	11.1	41.50	12.5	0.889	0.884

Keerthan and Mahendran (2011) developed suitable design equations for the shear capacity of LSBs (V_u) by including the available post-buckling strength (see Appendix). Shear capacities were calculated based on Keerthan and Mahendran (2011). The section moment capacities (M_u) for all FE models used in the parametric study were determined numerically using ABAQUS and the finite element model detailed in Anapayan and Mahendran (2009). Models used in the parametric study with aspect ratios of 2.0 and 2.5 typically displayed primary shear failure modes with well defined web yield zones. On average, 5%

and 12% reductions in shear capacity resulted from the presence of applied moments equivalent to 80% and 90% of the section moment capacities, respectively. It is important to note that only relatively small reductions in shear capacity resulted even when applied moments reached as high as 90% of the section moment capacity.

The finite element models with aspect ratios of 3.0, 3.5 and 4.0 were subject to bending moments equivalent to between 95% to 99% of their section moment capacities. All models within this range displayed predominantly bending failure modes characterised by buckling of the compression flange at mid-span and flange yielding which extended over much of the member length. Web yielding occurred locally at mid-span in all members subject to primary bending failure, which confirms that inelastic reserve capacity was mobilised at the ultimate load. On average, models used in the parametric study with aspect ratios of 3.0 were subject to shear forces up to 77% of their ultimate shear capacities. The corresponding reduction in bending moment capacity was on average 5%. At aspect ratios of 3.5 and 4.0, the magnitude of applied shear force dropped to 68% and 61% of the ultimate shear capacity, respectively. Such shear force magnitudes generally caused only minor reductions to bending capacity.

5. Comparison of Results with Australian Design Provisions

The results from this study were compared with AS/NZS 4600 and AS 4100 design provisions to determine their appropriateness for LSBs. Figure 9 shows the interaction between the shear and bending capacities of LSBs using the experimental and the corresponding FEA capacities. Shear test results from Keerthan and Mahendran (2011) were also included in the interaction diagram. It can be seen that AS/NZS 4600 provisions for combined shear and bending significantly underestimated the capacities of LSBs. As identified previously, such provisions are based on theory for disjointed plates in combined bending and shear, and are not accurate when applied to sections with rigid flanges. In contrast, predictions made using AS 4100 provisions compared reasonably well with the results obtained from FEA and experiments, which indicates that the combined shear and bending behaviour of the LSB is more consistent with that observed for hot-rolled steel sections. This is likely to be resultant of the stiff hollow flanges which contribute to a large proportion of the bending capacity much the same as the flanges in hot-rolled sections.

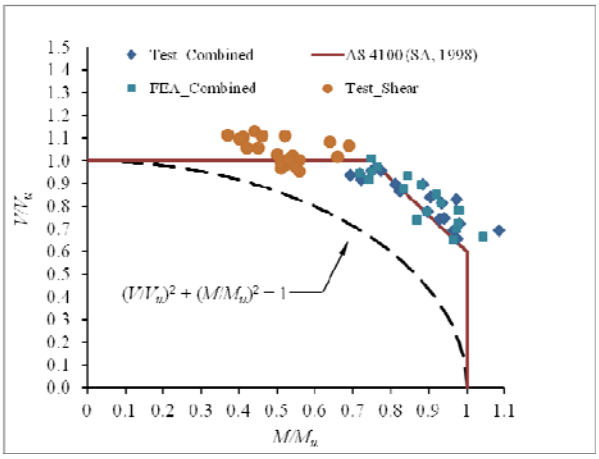

Figure 9: Interaction Diagram for LSBs Subject to Combined Shear & Bending

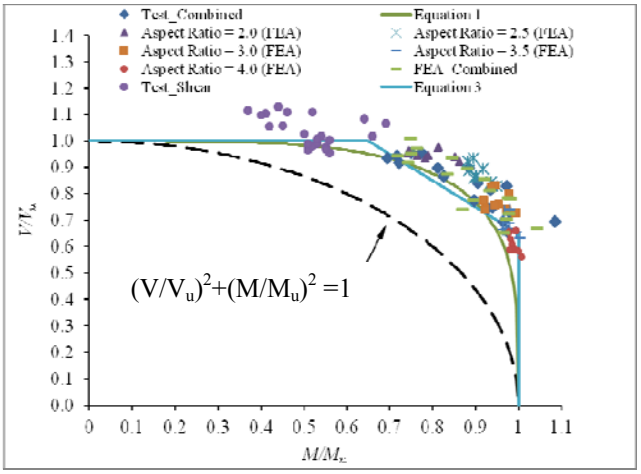

Figure 10: Proposed Interaction Diagram for LSBs Subject to Combined Shear and Bending

6. Proposed Equations for Combined Shear and Bending Action

The current Australian design code provisions are inadequate for predicting the combined shear and bending strengths of LSBs. Figure 10 shows the proposed

combined shear and bending interaction diagram for LSBs. All the capacity results for LSBs with aspect ratios of 2.0, 2.5, 3, 3.5, and 4.0 are now plotted in Figure 10. The results from the FEA and experimental studies were compared with current AS/NZS 4600 and AS 4100 design provisions. The overconservative nature of a circular interaction equation is clearly evident from Figures 9 and 10. In order to more accurately predict the capacities of LSBs under combined shear and bending actions, Equation 1 is proposed.

$$\left(\frac{M}{M_u}\right)^4 + \left(\frac{V}{V_u}\right)^4 \leq 1 \tag{1}$$

Equations 2 and 3 are also proposed as a linear alternative:

$$V = V_u \text{ for } \quad M < 0.65M_u \tag{2}$$

$$V = V_u\left[1.65 - \left(M / M_u\right)\right] \text{for} \, 0.65M_u \leq M \leq M_u \tag{3}$$

Equations 2 and 3 are proposed based on FEA and experimental results. These equations are linear equations as in AS 4100 (SA, 1998). M and V can be replaced by M^* and V^*, and likewise M_u and V_u can be replaced by $\phi_b M_s$ and $\phi_v V_v$ to produce equations that are consistent with AS/NZS 4600 provisions. It is interesting to note that Equation 1 is identical to that proposed by Shahabian and Roberts (2008) for plate girders. Again, this tends to indicate that LSB behaviour is more consistent with that of hot-rolled sections rather than typical cold-formed members.

The interaction diagrams shown in Figures 9 and 10 assume that section moment capacities are based on those from finite element analyses which include inelastic reserve capacity. Whilst the section moment capacities determined from finite element analysis are greater than those which would be calculated using the current AS/NZS 4600 provisions, the use of such values is justifiable given that they lead to more conservative capacity predictions.

7. Conclusions

This paper has described an investigation into the structural behaviour and design of LSBs subject to combined shear and bending actions using finite element analyses. Suitable finite element models were developed and validated by comparing their results with experimental test results. The developed nonlinear finite element model was able to predict the combined shear and bending capacities of LSBs and associated deformations and failure modes. Experimental and numerical studies showed that noticeable reductions in shear

capacity were observed when applied bending moments exceeded around 65% of the section moment capacity. Likewise, noticeable reductions in bending capacity were observed when applied shear forces exceeded around 65% of the shear capacity. The hot-rolled steel code (AS 4100) predictions compared reasonably well with the results from FEA and experiments, which reinforces that the behaviour of the LSB is more in line with that of hot-rolled sections. This is likely to be the effect of the stiff hollow flanges which contribute to a large proportion of the bending capacity as in hot-rolled beams. However, the cold-formed steel code (AS/NZS 4600) provisions were overly conservative for LSBs. Two lower bound equations were proposed to predict the capacities of LSBs subject to combined shear and bending actions.

Acknowledgements

The authors would like to thank Australian Research Council and OneSteel Australian Tube Mills for their financial support, and the Queensland University of Technology for providing the necessary facilities and support to conduct this research project. They would also like to thank Mr Ross Dempsey, Manager - Research and Testing, OneSteel Australian Tube Mills for his technical contributions, and his overall support to this research project.

References

Anapayan, T. Mahendran, M. and Mahaarachchi, D. (2011), Section Moment Capacity Tests of LiteSteel Beams, Thin-walled Structures, Vol.49, No.4, pp. 502-512.

Bleich, F. (1952), Buckling Strength of Metal Structures, McGraw Hill, New York, USA.

Evans, H. R. (1983), Longitudinally and Transversely Reinforced Plate Girders, In Plated Structures, Stability and Strength, Applied Science Publishers, London, UK.

Galambos, T. V. (1998), Guide to Stability Design Criteria for Metal Structures, 5th Edition, John Wiley and Sons, New York, USA.

Hibbitt, Karlsson and Sorensen, Inc. (HKS) (2007), ABAQUS User's Manual, New York, USA.

Keerthan, P. and Mahendran, M. (2010), Experimental Studies on the Shear Behaviour and Strength of LiteSteel Beams, Engineering Structures, Vol 32, pp. 3235-3247.

Keerthan, P. and Mahendran, M. (2011), New Design Rules for the Shear Strength of LiteSteel Beams, J. of Constructional Steel Research, Vol. 67, pp. 1050–1063.

LaBoube, R.A. and Yu, W.W. (1978), Cold-formed Steel Web Elements under Combined Bending and Shear, Research Report, American Iron and Steel Institute, University of Missouri-Rolla, Rolla, USA.

OneSteel Australian Tube Mills, (OATM) (2008), Design Manual of LiteSteel Beams, Australia.

Seo, J.K, Anapayan, T and Mahendran, M. (2008), Imperfection Characteristic of Mono- Symmetric LiteSteel Beams for Numerical Studies, Proc. of the 5th Int. Conference on Thin-Walled Structures, Brisbane, Australia, pp. 451-460.

Shahabian, F. and T. M. Roberts (2008), Behaviour of Plate Girders Subjected to Combined Bending and Shear Loading, Scientia Iranica, Vol 15, pp. 16-20.

Standards Australia/Standards New Zealand (SA) (2005), AS/NZS4600 Cold-Formed Steel Structures, Sydney, Australia.

Standards Australia/Standards New Zealand (SA) (1998). AS/NZS 4100 Steel Structures, Sydney, Australia.

Appendix : Proposed Design Equations for the Shear Strength of LSBs

$$\tau_v = \tau_{yw} \qquad \frac{d_1}{t_w} \le \sqrt{\frac{Ek_{LSB}}{f_{yw}}} \tag{4}$$

$$\tau_v = \tau_i + 0.25(\tau_{yw} - \tau_i) \qquad \sqrt{\frac{Ek_{LSB}}{f_{yw}}} < \frac{d_1}{t_w} \le 1.508\sqrt{\frac{Ek_{LSB}}{f_{yw}}} \tag{5}$$

$$\tau_v = \tau_e + 0.25(\tau_{yw} - \tau_e) \qquad \frac{d_1}{t_w} > 1.508\sqrt{\frac{Ek_{LSB}}{f_{yw}}} \tag{6}$$

where

$$\tau_{yw} = 0.6 f_{yw} \qquad \tau_i = \frac{0.6\sqrt{Ek_{LSB} f_{yw}}}{\left[\frac{d_1}{t_w}\right]} \qquad \tau_e = \frac{0.905 Ek_{LSB}}{\left[\frac{d_1}{t_w}\right]^2} \tag{7}$$

$$k_{LSB} = k_{ss} + 0.87(k_{sf} - k_{ss})$$